Satellite Application Facility on Climate Monitoring

Algorithm Theoretical Basis Document

Total Column Water Vapour Retrieval from SSM/I (HTW_SSMI, version 3.1)

Reference Number:	**SAF/CM/DWD/ATBD/HTW_SSMI**
Issue/Revision Index:	**1.1**
Date:	**06 January 2009**

Document Signature Table

	Name	Function	Signature	Date
Author	Markus Jonas	CM-SAF scientist		06/01/09
Editor	Jörg Schulz	Science Coordinatior		06/01/09
Approval	Martin Werscheck	Project Manager		06/01/09
Release				
Eumetsat Approval	Lothar Schueller	EUMETSAT SAF coordinator		

Distribution List

Internal Distribution	
Name	**No. Copies**
DWD Archive	1
CM-SAF Team	1

External Distribution		
Company	**Name**	**No. Copies**
PUBLIC		

Document Change Record

Issue/ Revision	Date	DCN No.	Changed Pages/Paragraphs
1.0	31/10/08	SAF/CM/DWD/ATBD/WVPA_HO	Initial release
1.1	06/01/09	SAF/CM/DWD/ATBD/WVPA_HO	Implemented recommended changes due to DRI

Table of Contents

1. INTRODUCTION 4
1.1. Applicable Documents 5
2. ALGORITHM OVERVIEW 5
3. ALGORITHM DESCRIPTION 5
3.1. Theoretical Description 5
3.1.1. Radiative Transfer 6
3.1.2. Retrieval scheme 9
3.1.3. Error Budget Estimates 10
3.2. Practical Application 10
4. ASSUMPTIONS AND LIMITATIONS 12
5. REFERENCES 14

List of tables

Table 1: Spectral characteristics of the SSM/I instruments aboard the DMSP satellites. 5
Table 2: Regression coefficients, explained variance and retrieval accuracy for the four regression algorithms tested by Schlüssel and Emery (1990). Their table 3, modified. 10

List of figures

Figure 1: Microwave attenuation of water vapour and oxygen (after Liebe, 1985). 7
Figure 2: Scatter plots between input water vapour column content (x-axis, in g/cm), for the simulated SSM/I channels 19 GHz (top left), 22 GHz (top right), 37 GHz (bottom left) and 85 GHz (bottom right). All simulated brightness temperatures are for vertical polarization (reprinted from Schlüssel and Emery (1990), Fig. 1). 8
Figure 3: Histograms of differences in retrieved water vapour content for the retrievals tested. All panels use retrieval Nr 4 (cf Table 2) as reference. Left panel shows the difference to approach Nr 1 (cf Table 2), middle panel to approach Nr 2 (cf Table 2), and right panel to approach Nr 3 (cf Table) (reproduced Fig. 5 from Schlüssel and Emery (1990)). 11
Figure 4: Differences between true water vapour content from radiosondes and water vapour content obtained from retrieval scheme Nr 4 (cf Table 2) from SSM/I (from Schlüssel and Emery (1990), Fig. 3). 13

1. Introduction

This CM-SAF Algorithm Theoretical Basis Document (ATBD) provides information on the CM-SAF total column water vapour (WVPA) retrieval scheme used to construct the data set employing Special Sensor Microwave/Imager (SSM/I) observations onboard Defence Meteorological Satellite Program (DMSP) platforms F08, F10, F11, F13, F14 and F15. The same algorithm has already been used in the Hamburg Ocean-Atmosphere Parameters and Fluxes from Satellite (HOAPS, www.hoaps.org) data set (Schulz et al. 1998, Jost et al. 2002, Andersson et al. 2008). The document gives background information on the physics of the problem, the training and derivation of the statistical inversion scheme and consideration of constraints and limitations of this retrieval.

More information on the data set is contained in the product user manual (PUM) [AD 2], basic accuracy requirements are defined in the product requirements document (PRD) [AD 1], and the validation of the data set versus those requirements is described in the validation report [AD 3].

The HOAPS data set contains multiple parameters derived from SSM/I observations. The complete set of HOAPS parameters consists of the following atmospheric and near-surface variables, derived for the global ice-free oceans:

- **Vertically integrated water vapour**
- Vertically integrated total (ice+liquid) water
- Vertically integrated liquid water [*]
- Wind speed at 10m height [*]
- Near surface specific humidity [*]
- Precipitation [*]
- Sea surface temperature [*] (from AVHRR, provided for consistency)
- Sea surface saturation specific humidity [*]
- Long wave net flux at sea surface
- Difference in specific humidity
- Latent heat transfer coefficient (Dalton number)
- Latent heat flux at sea surface [*]
- Sensible heat flux at sea surface
- Evaporation [*]
- Freshwater flux [*].

Variables marked by [*] will become CM-SAF products with future releases of the HOAPS data set. The scope of this document is to describe the algorithm incorporated in the HOAPS software that derives water vapour (bold typesetting).

A description of the parameters, their dependency on additional input data sources, their continuation with furture HOAPS releases and the HOAPS versioning approach is given in the product user manual (PUM) [AD 2].

1.1. Applicable Documents

Reference	Title	Code
AD 1	CM-SAF Product Requirements Document	SAF/CM/DWD/PRD/1
AD 2	Product User Manual HTW_SSMI_global_DS	SAF/CM/PUM/ HTW_SSMI_global_DS
AD 3	Validation Report HTW_SSMI_global_DS	SAF/CM/VAL/DRI-1

2. Algorithm Overview

The algorithm used to derive total column water vapour from SSM/I observations has been developed by Schlüssel and Emery (1990). It is a semi-physical retrieval based on radiative forward calculations and statistical inversion. Several versions of the retrieval have been developed by Schlüssel and Emery (1990) but only one emplyoing two channels (22 and 37 GHz vertical polarisation) has been used to construct the HOAPS data set. The following table lists all channels of the SSM/I instruments, the two channels used are marked by bold typesetting. For more details on the SSM/I instrument, see Hollinger et al. (1987).

Radiative transfer, training data base used for the derivation of the inversion parameters, retrieval algorithm, its application to the SSM/I data, and informatiion on known limitations of the algorithm are described in the following subsections.

Table 1: Spectral characteristics of the SSM/I instruments aboard the DMSP satellites.

* The ground resolution is based on the 3dB antenna footprint and the integration time of ~ 8 ms.

channel	*frequency (GHz)*	*polarization*	*ground resolution (km) **
1	19.35	vertical	~ 70
2	19.35	horizontal	~ 70
3	**22.235**	**vertical**	**~ 60**
4	**37.0**	**vertical**	**~ 50**
5	37.0	horizontal	~ 50
6	85.5	vertical	~ 15
7	85.5	horizontal	~ 15

3. Algorithm Description

3.1. Theoretical Description

Microwave radiometry is very much suited to derive water vapour columns, as the thermal radiation at millimetre and centimetre wavelengths emerging from both the surface of the earth and the atmosphere is penetrating all but the very optically thick and raining clouds.

Additionally, the emission of the sea surface is rather small so that the emission signal from atmospheric water vapour can easily be distinguished from the surface signal at 22 GHz.

The CM-SAF algorithm approach follows that from Schlüssel and Emery (1990) to derive the water vapour retrieval for SSM/I. It consists of the following steps:

1. Identify atmospheric and surface state variables that are needed to describe the radiative transfer in the microwave part of the electromagnetic spectrum.
2. Depict the atmospheric and surface variability in terms of those variables by a representative data base of observed atmospheric profiles and surface properties.
3. Apply a radiative transfer code to obtain synthetic SSM/I radiances from the input profiles and surface conditions.
4. Perform a correlation analysis between those synthetic radiances and the input water vapour column content for the SSM/I channels.
5. Identify the channel combinations explaining most of the variance present in the atmospheric profiles and perform linear regression analysis to derive coefficients for these channel combinations.
6. Apply the retrieval coefficients to a selected period of SSM/I observations and compare the obtained water vapour values to radio soundings not contained in the training data set to evaluate the accuracy of the retrieval.

3.1.1. Radiative Transfer

The radiative transfer is approximated by the following equation (1):

$$I_\nu = \epsilon_\nu B_\nu(T_s)\tau_\nu^* + \int_{p_s}^{0} B_\nu(T)\frac{\partial \tau_\nu}{\partial p}dp + (1-\epsilon_\nu)\tau_\nu^* \int_0^{p_s} B_\nu(T)\frac{\partial \tau_\nu}{\partial p}dp \qquad (1)$$

where ν is frequency, T is temperature, T_s is surface temperature, ε_ν is surface emissivity, B_ν is the Planck function, p is pressure, p_s is surface pressure, τ_ν is transmission and τ_ν* is total atmospheric transmission. The three right-hand terms may be interpreted as follows:

– the first term gives the proportion of surface emission at temperature T_s and emissivity ε_ν, transmitted through the atmosphere with transmissivity τ_ν*.

– the second term describes the upwelling emitted radiation of the atmosphere integrated from the surface to the top (in pressure coordinates). The emission $B_\nu(T)$ is weighted by the vertical derivative of transmission as function of atmospheric pressure.

– the last term describes the downwelling atmospheric radiation that is reflected at the surface with the reflectivity 1-ε_ν and transmitted through the atmosphere with the total transmissivity τ_ν*. Note that for this, it has been assumed that $\varepsilon_\nu + \rho_\nu = 1$, i.e. the penetration depth of radiation for the SSM/I channel wavelengths has been set to zero which is a reasonable approximation.

The solution of the radiative transfer equation in the microwave part of the spectrum requires a description of the transmission of the atmosphere and the quantification of the surface emission. As the atmospheric transmissivity is concerned, water vapour and oxygen are – apart from hydrosols – the relevant absorbers as is shown in Figure 1 for the spectral range of SSM/I observations. The extinction coefficients at varying atmospheric conditions have been fully described by Liebe (1985), whose attenuation model is adopted here. Optical depth has been computed for 22 homogeneous vertical layers in which atmospheric profiles could be introduced. The radiosonde data base used covers all necessary input parameters such that the forward radiative transfer can be computed.

Hydrometeors do also affect the atmospheric transmissivity by scattering. As this process is not covered by the radiative transfer model applied for the retrieval of total column water vapour, atmospheric conditions including heavy rain have to be filtered out prior to the application of the algorithm.

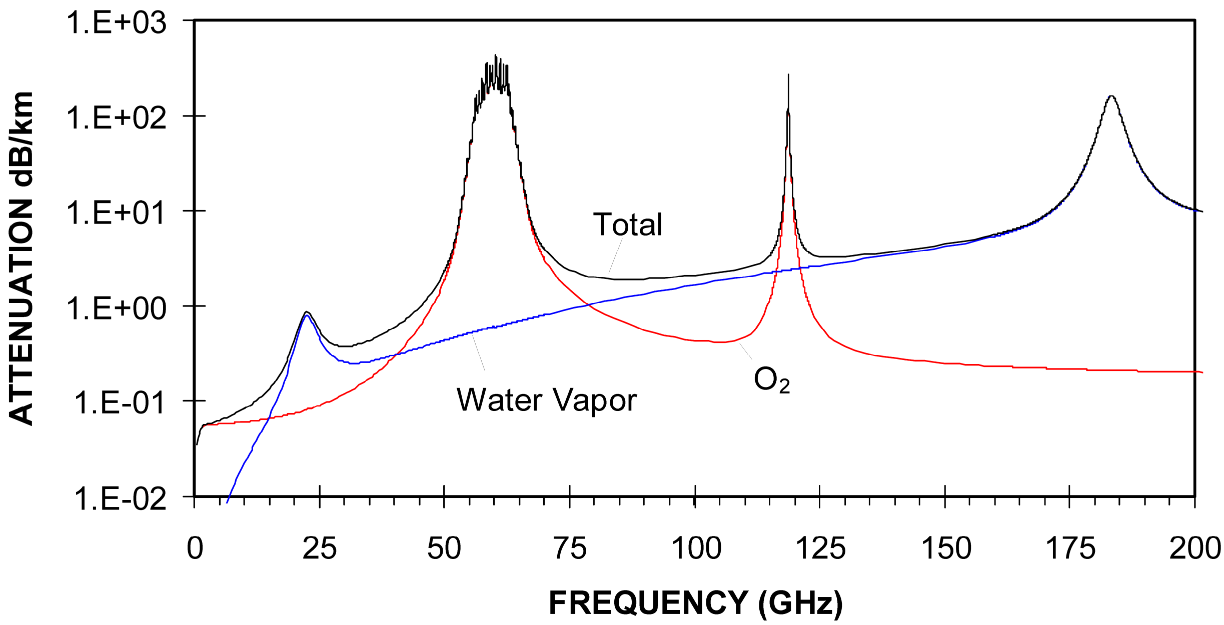

Figure 1: Microwave attenuation of water vapour and oxygen (after Liebe, 1985).

To determine the surface emission surface temperature, salinity, and roughness have to be known. The description of the surface emissivity is done in a two-step calculation. First, surface temperature and salinity are used to calculate the complex dielectric constant for sea water which then fits into the Fresnel formulae to obtain the emissivity of a planar surface. Adaptations for a rough surface are made in a second step. Roughness is introduced by waves and also by foam covering the surface which are both treated by an empirical model by Wentz (1983) using friction velocities derived from surface wind speeds as input. This parametrization had originally been derived for SMMR (Scanning Multichannel Microwave Radiometer aboard Seasat). Coefficients for the different central wavelengths of the SSM/I channels have been interpolated using Wentz' coefficients, the SMMR channel wavelengths and a cubic spline interpolation.

The reference data base for the forward calculations consists of 288 oceanic atmospheres for all seasons collected from oceanic radiosonde ascents. Profiles contain water vapour and temperature information and are complemented by surface temperature, salinity and surface winds. Additionally, clouds have been randomly introduced into the profiles by setting liquid-water contents using a normal distribution (with mean 2 kg/m² and standard deviation 3 kg/m²). The coupling with the water vapour profile was done such that the maximum liquid water content allowed in one layer was restricted to half the water vapour content of that layer. Values below zero were set to no-cloud conditions. Cloud thickness was assumed to be at least 50hPa. This yields an integrated liquid water vapour content of max. 1.4 kg/m² which does not cover the spectrum of clouds occurring. Larger values may occur in heavy precipitating clouds, for which the approximation of radiative transfer used is not valid. Those situations are excluded from the simulation.

Sea surface temperature has been set by varying the lowermost air temperature with a normally distributed noise function of 3 K amplitude. A threshold of -1.9℃ for the lowermost allowed ice-free ocean SST has been assumed and all temperature values below have been set to that threshold value. Sea surface salinity has been fixed to 35‰ which is reasonable as the influence of sea surface salinity is rather small at SSM/I frequencies. Surface wind information is added as friction velocities that were randomly varied with a mean of 0.25 m/s and a standard deviation of 0.3 m/s, where negative values have been set to zero-wind conditions.

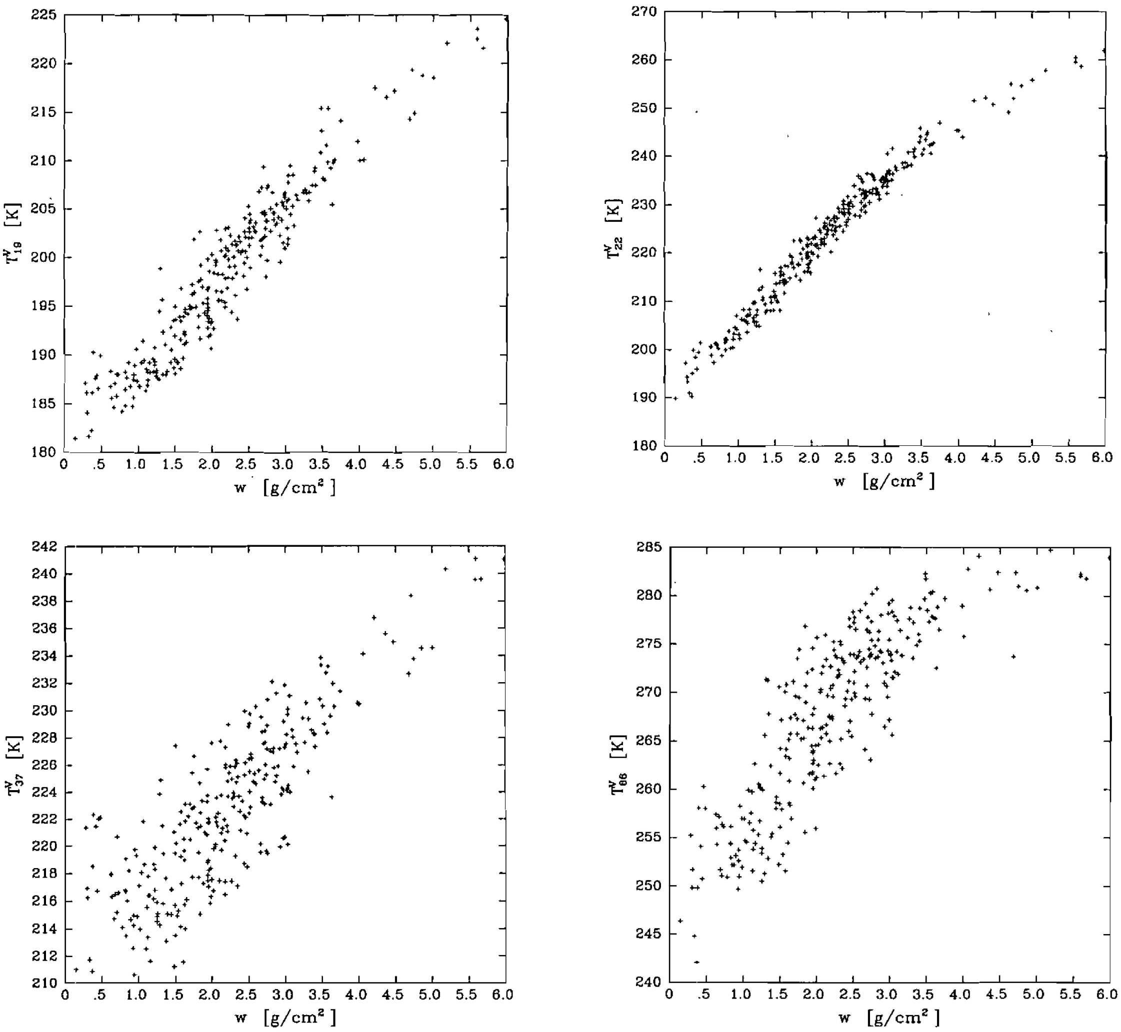

Figure 2: Scatter plots between input water vapour column content (x-axis, in g/cm), for the simulated SSM/I channels 19 GHz (top left), 22 GHz (top right), 37 GHz (bottom left) and 85 GHz (bottom right). All simulated brightness temperatures are for vertical polarization (reprinted from Schlüssel and Emery (1990), Fig. 1).

After the forward simulation, the obtained radiances have been converted to brightness temperatures using the Rayleigh-Jeans approximation. Instrumental noise represented by a normally distributed noise function with a zero mean and a standard deviation of the noise equivalent difference temperatures as specified by Hollinger et al. (1988) for the SSM/I instrument channels has been added after the conversion into brightness temperatures.

3.1.2. Retrieval scheme

The simulated brightness temperatures have been analysed versus the known input water vapour column values. In all cases, the simulated brightness temperature increases with increasing water vapour. This functional dependence is closest for the 22 GHz channel, as can be seen from the following Figure 2, where in the upper right panel the scatter is smallest. This is in accordance with the laboratory spectroscopy shown in Figure 1, as the 22 GHz channel is centered at the water vapour absorption line. Thus, one should expect the tightest relation between water vapour content and simulated brightness temperature here.

The brightness temperatures for the 22 GHz reveal a nice linear relationship to the water vapour column contents up to 30 kg/m², at higher values a slight saturation of the signal can be observed. In the other channels, the enhanced scatter basically stems from increased surface emission contributions to the radiometer signal.

As has been shown beforehand, the 22 GHz channel contains most information on the atmospheric water vapour contents. The simulated brightness temperatures for that channel were therefore used to train the statistical retrieval. Mathematically, a multiple linear regression between water vapour content and simulated brightness temperature has been carried out. This requires a linearization of the relationship. Chang and Wilheit proposed in 1979 to use a logarithmic function of type WVPA ~ $ln(280 - T_{22})$ which has also been applied by Schlüssel and Emery (1990).

In order to minimize the not explained variance by this simple functionality using only one channel, Schlüssel and Emery (1990) also used multi-channel approaches to correct effects due to surface roughness and cloud water content. In total, they tested four regression schemes given by the following equations:

$$w_a = a_0 + a_1 ln(280 - T_{22}) \tag{2}$$

$$w_b = b_0 + b_1 ln(280 - T_{22}) + b_2[T_{19} - ln(280 - T_{22})] \tag{3}$$

$$w_c = c_0 + c_1 ln(280 - T_{22}) + c_2[ln(280 - T_{22}) - T_{37}] \tag{4}$$

$$w_d = d_0 + d_1 ln(280 - T_{22}) + d_2(T_{37} - T_{86}^{0.8}) \tag{5}$$

The first regression purely relates the linearised 22 GHz channel brightness temperature to the total coloumn water vapour. The second scheme also employs the brightness temperature difference between the 22 and 19 GHz channel. The third formula employs the difference between the 22 and 37 GHz channel and finally the last regression scheme that one between 37 and 85 GHz. Table 2 shows the regression coefficients derived from the simulated brightness temperatures, the explained variance by the corresponding equation and the statistical accuracy of the retrieval.

Table 2: Regression coefficients, explained variance and retrieval accuracy for the four regression algorithms tested by Schlüssel and Emery (1990). Their table 3, modified.

Retrieval	Regression coefficient I=0	1	2	Explained variance [%]	Accuracy [kg/m²]
1	16.53	-3.576	--	98.70	1.7
2	22.15	-4.116	-0.001777	98.85	1.6
3	23.82	-4.059	0.02451	98.99	1.5
4	22.73	-3.969	-0.03423	99.05	1.45

The statistics show that the explained variance of the single channel approach is already quite high. The increase in explained variance by including other channels is on the order of 0.3 %. Only the inclusion of the 85 GHz channel achieves an explained variance of more than 99%. Schlüssel and Emery (1990) also tested a retrieval using all SSM/I channels simultaneously and found that this approach did not enhance explained variance any further but increased the numerical instability due to multi-collinearity effects.

From a scientific point of view, the retrieval using the 22 and 85 GHz channels (cf Table2, Nr 4) would thus be the optimum retrieval of all combinations tested. Nevertheless, the 85 GHz channel failed aboard the F-08 satellite and would have to be synthetically generated for retrieval purposes. The synthesis of a channel would introduce an additional source of uncertainty such that retrieval Nr 3 (cf Table 2) employing the 22 and 37 GHz channels has been chosen for application in CM-SAF.

3.1.3. Error Budget Estimates

Based on the evaluation of the explained and residual variance, the accuracy of the inversion for retrieval Nr 3 can be specified as 1.5 kg/m² (cf. Table 2). This error contains all uncertainties present in the derivation of the retrieval algorithm, the assumptions made and the models and data used. As the inversion is of statistical nature the error budget cannot be subdivided.

3.2. Practical Application

Schlüssel and Emery (1990) have applied their retrieval coefficients to a selected period of four days in 1987. Prior to the application of the retrieval, several instrument calibrations described in Wentz (1988) and a conversion from the antenna radiances to brightness temperatures (also Wentz, 1988) have been performed. Derived water vapour contents from 52 DMSP orbits corresponding to 4 days of data were averaged into 0.25° x 0.25° grid boxes. Indvidual radio soundings from ships were attached to those grid box values resulting in 240 matchups. All retrieval schemes given in Table 2 were applied and systematic and random differences to the radiosondes were investigated.

As the theoretical approach chosen by Schlüssel and Emery (1990) did not include scattering due to hydrometeors, such atmospheric conditions have to be filtered out prior to the retrieval. During their study to derive the statistical WVPA retrieval, this was done via a two-step threshold criterion in brightness temperature space. First, all measurements with brightness temperatures of the 85 GHz channel outside the 240-290 K range are excluded and second. observations with temperature differences (85 GHz minus 37 GHz) outside 5 - 55 K are excluded. By these threshold criteria, situations containing rain and high liquid water amounts are reliably filtered. The practical application of the rain-screening within the HOAPS data set is slightly different. The retrievals for all parameters (see section 1) are run sequentially. The computation of near-surface parameters and budgets is only possible if parameter wind and WVPA are simultaneously defined (i.e. they should be based on the same screening approaches). The wind retrieval in HOAPS also requires a rain screening, which is slightly more restrictive than the one by Schlüssel and Emery (1990) described above. In the wind retrieval, the following three thresholds are applied: (1) the brightness temperature of the 19 GHz channel (hor.) must be less than 185 K, (2) the temperature difference between the 37 GHz and 19 GHz channels (both hor.) must be less than 40 K and (3) the polarization difference in the 37 GHz channel (vert. minus hor.) must be greater than 35 K. As mentioned, the number of pixels rejected by these criteria is slightly higher than the number by the Schlüssel and Emery two-threshold screening (i.e. rain-screened pixels by the wind algorithm are a superset of those rain-screened by the WVPA retrieval). The wind retrieval is run first, and the following WVPA retrieval is only kicked off if the wind retrieval yields “rain-free” conditions.

The application of the retrieval scheme and comparison to radio soundings showed a bias of 0.81 kg/m² for the simple one-channel approach. Applying retrieval Nr 4 (cf Table 2) Schlüssel and Emery (1990) found a reduced bias of only 0.23 kg/m² and a corresponding standard deviation of 5.6 kg/m².

Schlüssel and Emery (1990) further discussed the global biases between the four retrieval schemes and the results are displayed in Figure 3. The mode in the histograms is found to be slightly positive in the first two comparisons, the negative tail is in all cases longer than the positive one. The approach using the 22 and 37 GHz channels (Nr 3, cf Table 2) is closest to the reference multi-channel retrieval Nr 4 (Table 2) as is shown by the very narrow, short-tailed and zero-centered histogram in the right panel of Figure 3. This again justifies the selection of this algorithm for practical reasons, as the 85 GHz channel is not available for all SSM/I instruments and types.

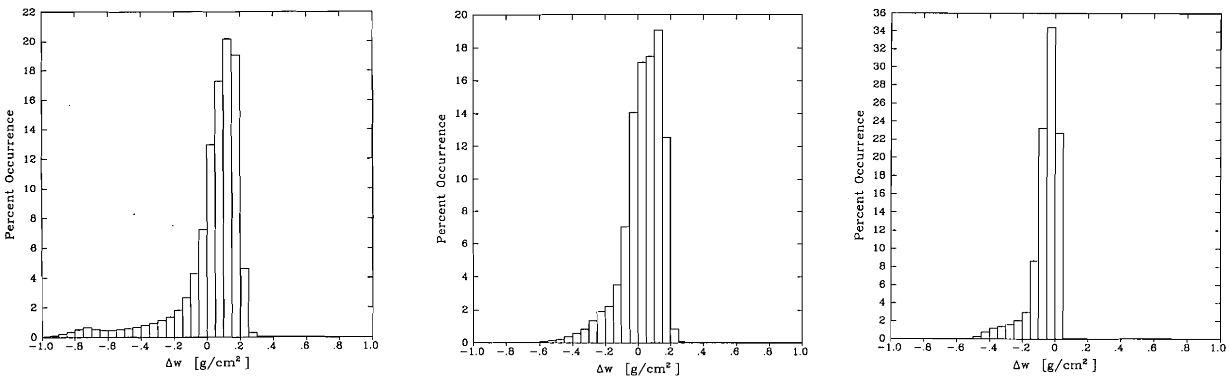

Figure 3: Histograms of differences in retrieved water vapour content for the retrievals tested. All panels use retrieval Nr 4 (cf Table 2) as reference. Left panel shows the difference to approach Nr 1 (cf Table 2), middle panel to approach Nr 2 (cf Table 2), and right panel to approach Nr 3 (cf Table) (reproduced Fig. 5 from Schlüssel and Emery (1990)).

The value found for the standard deviation seems to be very large, but includes multiple sources of uncertainty as retrieval errors, errors due to spatial and temporal mismatches, errors due to undetected high liquid-water contents as well as errors in radiosonde observations. In addition, the variability of the total column water vapour during the four days also accounts for the large difference. The averaged variability computed as the local standard deviation in each of the 240 0.25°x 0.25° grid boxes was found to be 5.4 kg/m².

4. Assumptions and Limitations

As outlined in the description of the algorithm derivation the underlying regression technique is based on the following assumptions:

- The radiative transfer model used for the simulation of the SSM/I brightness temperatures covers all relevant processes and input variables.

- The true atmospheric variability of all needed input variables to the radiative transfer model is adequately represented in the 288 profiles contained in the training data base.

As the radiative transfer calculations did not include scattering due to hydrometeors, the derived retrieval may only be applied for non-rain conditions, i.e. a rain-screening is applied beforehand.

Sohn and Smith (2003) showed in a study comparing different statistical retrieval methods for water vapour content from SSM/I observations, including the Schlüssel and Emery algorithm, that (a) systematic differences in the derived water vapour contents exist and that (b) those may be significantly reduced by a re-training of the regression scheme with a common training data base. This leads to the conclusion that the second assumption mentioned above is crucial for the development of a statistical inversion scheme. However, they also showed that the initial difference prior to the re-training between the Schlüssel and Emery (1990) algorithm and an optimum statistical retrieval (Wentz 1995) considered as reference was close to zero and the smallest of all retrievals considered. The latter is an indication that the Schlüssel and Emery (1990) training data set fulfils the assumption of representing true atmospheric variability to a satisfying amount. Details on the intercomparison study by Sohn and Smith (2003) and the associated uncertainties of the CM-SAF WVPA data set are described in detail in the validation report [AD 3].

The training data base used covered water vapour values between 2 kg/m² and 60 kg/m² with a mean of 22 kg/m². A detailed assessment of the standard error of the retrieval binned by water vapour values showed that especially at very low water vapour values (cold and dry polar atmospheres) the error of the retrieval may reach 100%. This is due to the fact that in those very cold atmospheres the total column water vapour is very much determined by the temperature profile which cannot be adequately reproduced with the radiative transfer model used as this model consists only of 22 vertical layers. Thus, the retrieval tends to systematically overestimate the water vapour at very cold and dry atmospheres. Figure 4 shows the difference between the true water vapour content from the training radiosondes and the retrieved water vapour content as a function of the water vapour content (negative values indicate an overestimation by the retrieval). For water vapour contents less than 6 kg/m² only overestimations of up to 3 kg/m² occur. Similar results have been found in the validation of the final CM-SAF WVPA data set and are presented in the validation report [AD 3]. This deficiency can be corrected by a redevelopment of the retrieval scheme for the atmospheric parameters of the HOAPS data set.

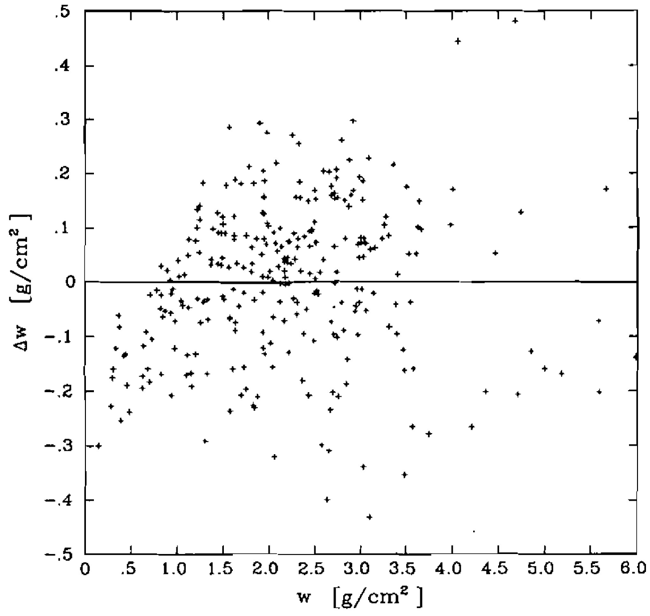

Figure 4: Differences between true water vapour content from radiosondes and water vapour content obtained from retrieval scheme Nr 4 (cf Table 2) from SSM/I (from Schlüssel and Emery (1990), Fig. 3).

5. References

Andersson, A., C. Klepp, K. Fennig, S. Bakan, H. Grassl, and J. Schulz, 2008: The HOAPS climatology: Essential water cycle components over global oceans derived from satellite data. submitted to Bull. Amer. Meteor. Soc.

Chang, A.T. and T.T.Wilheit, 1979: Remote sensing of atmospheric water vapour, liquid water and wind speed at the ocean surface by passive microwave techniques from the NIMBUS 5 satellite. Radio Science, **14**, 793-802.

Hollinger, J.P., Lo, R., Poe, G., Savage, R. and Peirce, J. 1987: Special Sensor Microwave/Imager User's Guide (Washington D.C., Naval Research Laboratory).

Jost, V., S. Bakan and K. Fennig 2002: HOAPS – A new satellite-derived freshwater flux climatology. Meteorol. Zeitschrift, **11**, 61-70.

Liebe, H.J., 1985: An updated model for millimetre wave propagation in moist air. Radio Science, **20**, 1069-1089.

Schlüssel, P. and W.J. Emery 1990: Atmospheric water vapour over oceans from SSM/I measurements. Int. J. Remote Sensing, **11**, 753-766.

Schulz, J., V. Jost and S. Bakan 1998: A new satellite-derived freshwater flux climatology (Hamburg Ocean Atmosphere Parameters and Fluxes from Satellite). International WOCE Newsletter, **32**, 20-26.

Sohn, B.J. and E.A. Smith 2003: Explaining sources of discrepancy in SSM/I water vapour algorithms. Journal of climate, **16**, 3229-3255.

Wentz, F.J., 1983: A model function for ocean microwave brightness temperatures. Journal Geophys. Res. **98**, C3, 1892-1908.

Wentz, F.J., 1988: User's Manual SSM/I Antenna Temperature Tapes (Tech. Rep. 032588), Remote Sensing Systems, Santa Rosa, California, available via www.remss.com

Wentz, F.J., 1995: The intercomparison of 53 SSM/I water vapour algorithms. Remote Sensing Systems Tech. Rep. on WetNet Water Vapour Intercomparison Project (VIP), Remote Sensing Systems, Santa Rosa, California, available via www.remss.com